# Jointly Optimal Design for MIMO Radar Frequency-Hopping Waveforms Using Game Theory

**KEYONG HAN,** Student Member, IEEE
**ARYE NEHORAI,** Fellow, IEEE
Washington University in St. Louis
St. Louis, MO, USA

**Using a colocated multiple input/multiple output (MIMO) radar system, we consider the problem of joint design of amplitudes and frequency-hopping codes for frequency-hopping waveforms. The joint design method yields better combined code and amplitude matrices that result in improved performance over that of separate designs. We propose a game theory framework for the joint design. First, we present the MIMO radar signal model and the sparse representation. Then the problem formulation is constructed based on sparse recovery and the ambiguity function of the MIMO radar system for frequency-hopping waveforms. For amplitude design, we propose two strategies: amplitude design with separate constraints and amplitude design by fusing all transmitters. We formulate a novel game model and propose two joint design algorithms, one applying a noncooperative scheme and the other applying a cooperative scheme. Owing to the extremely large size of the feasible set of the discrete code, we propose to use these algorithms to obtain the $\epsilon$-approximate equilibrium. We demonstrate the improvement of the resulting codes and amplitudes through numerical examples.**

Manuscript received May 30, 2014; revised May 4, 2015; released for publication September 29, 2015.

DOI. No. 10.1109/TAES.2015.140408.

Refereeing of this contribution was handled by G. San Antonio.

This work was supported by the AFOSR Grant FA9550-11-1-0210 and ONR Grant N000141310050.

Authors' address: Preston M. Green Department of Electrical and Systems Engineering, Washington University in St. Louis, St. Louis, MO, 63130. Corresponding author is A. Nehorai, E-mail: (nehorai@ese.wustl.edu.).



## I. INTRODUCTION

Multiple input/multiple output (MIMO) radar [1–6] is an active technology that is attracting the attention of researchers due to the improvement in performance it offers over conventional single antenna systems. In the traditional standard phased-array radar, the system transmits only scaled versions of a single waveform. The MIMO radar system allows transmitting multiple probing signals that may be chosen quite freely, obtaining more degrees of freedom than systems with a single transmit antenna [7]. MIMO radar systems are commonly used in two different antenna configurations: distributed [2] and colocated [3]. Both distributed and colocated MIMO radars exploit waveform diversity, and it has been shown that both radars have many advantages. In this paper, whenever we mention MIMO radar, we are referring to colocated MIMO radar.

The frequency-hopping waveforms, proposed in [8], were originally designed for multiuser communications, radar, and sonar systems. Because frequency-hopping signals can be easily generated and have constant modulus, they have been considered effective radar waveforms. In [4–6], the authors used the frequency-hopping codes to exploit waveform diversity for colocated MIMO radar and considered adaptive waveform design. The MIMO ambiguity function is used to optimize the frequency-hopping codes in [5], with the assumption that the target Dopplers are small. The extension of the small Doppler condition to the general case was conducted in [4], which applied the hit-matrix formalism to design the code matrix. Both frequency-hopping code and amplitude designs are considered in [6] by using sparse modeling, but they were designed separately. Our goal in this paper (see also [9]) is to jointly design the codes and amplitudes.

Multiobjective optimization problems can be found in various fields, wherever optimal decisions need to be made in the presence of trade-offs between two or more conflicting objectives. Various methods have been studied to solve such problems [10]. Methods that transform multiple objective functions into a single one include the weighted sum method, lexicographic method, and physical programming. Other approaches, such as genetic algorithms [11, 12], can be used to solve multiobjective problems directly but perform badly when the function evaluation is expensive. In recent years, game theory has been used to solve multiobjective design problems, especially for some practical problems in engineering [13]. Rao [14] proposed a game based on Nash equilibrium to conduct optimization problems and described the relationship between Pareto-optimal solutions and game theory. Applications of game-based methods to solve multiobjective optimization problems in some engineering examples can be found in [15, 16].

Frequency-hopping waveform design has been widely studied recently for both frequency codes and amplitudes. Gogineni and Nehorai [6] formulated two objective functions based on the sparse model. The objective function for amplitude matrix $\boldsymbol{B}$ is related to the code matrix, denoted as $\boldsymbol{C}$. However, the objective function for $\boldsymbol{C}$, developed based on block coherence, is independent of $\boldsymbol{B}$, which makes it difficult for us to apply game theory to solve this joint problem. The frequency-hopping waveforms used in [5] based on the ambiguity function made the assumption that the amplitudes for all transmitters and frequencies are the same. We generalize this by considering various amplitudes, and the resulting objective function is naturally involved with the amplitudes. The optimal code design based on ambiguity function obtains good resolution, and the amplitude design based on sparse recovery improves the detection performance. It is natural for us to combine these two objective functions, exploiting the advantages of both designs. We propose to employ game theory to solve this joint optimization problem by viewing the two objective functions as two interacting players. We will show that the joint design improves the performance of both matrices at the same time. Note that, in [6], the authors used the strategy of amplitude design with separate (ADS) constraints, which assigned the same energy constraint to each transmitter. However, in practice, it makes more sense to use a sum of the transmitted energy constraint across all transmitters. That is, different transmitters may have different energies, depending on their respective channel qualities. Therefore, we propose another strategy, amplitude design by fusing (ADF) all transmitters. We will show the comparative results of these two strategies through numerical examples.

The formulated game combines players whose strategy spaces consist of both discrete set and continuous set. The size of the feasible space for code matrix is highly dependent on the numbers of transmitter $M_T$ and frequency-hopping choice $K$. Because the code feasible space will become extremely large as $M_T$ or $K$ increases, it is almost impossible for us to find the Nash equilibrium due to the expensive computational cost. However, the simulated annealing [17] algorithm helps us to find an approximate optimal solution for the single code objective function, leading to an $\epsilon$-approximate equilibrium ($\epsilon$-AE) [18] for the joint problem.

Building on our previous conference paper [9], we have added quite a few new points: for the amplitude objective function, we have constructed a more effective strategy by fusing all transmitters' information (ADF); for the game model, we have elaborated the detailed definition of the $\epsilon$-AE; for the optimization, we have provided insightful analysis of the convergence performance of the proposed algorithms; and last but not least, we have investigated far more numerical examples to illustrate the effectiveness of our algorithms.

The rest of this paper is organized as follows. In Section II, we present the signal model for the colocated MIMO radar, including the measurement model and the sparse model. The game model formulation, together with two joint design algorithms based on game theory, one applying a noncooperative scheme and the other applying a cooperative scheme, is stated in Section III. In Section IV, we use numerical results to show the advantage of our joint design over the separate design. Our conclusions and directions for possible future work are contained in Section V.

## II. SIGNAL MODEL

In this section, we will describe the signal model for our radar system. We first develop the measurement model for MIMO radar estimation problem. Then we transform the measurement model to a sparse representation.

### A. Measurement Model

We assume that there are $M_T$ transmitters and $M_R$ receivers in the colocated MIMO radar system, arranged in uniform linear arrays. The spacing between the transmitters is $d_T$, and the spacing between receivers is $d_R$. Additionally, we assume that the targets are at far-field with respect to the radar, i.e., the direction of propagation is approximately equal at each sensor. Also, we assume the relative distance between any two targets is much smaller than their individual distances with respect to the radar. Hence, all the targets can be associated with the same direction-of-arrival [5, 6, 19]. Let these arrays form the same angle $\theta$ with the targets. Let $L$ pulses comprise a waveform, and we can write the frequency-hopping waveform from the $m$th transmitter as

$$u_m(t) = \sum_{l=0}^{L-1} \phi_m(t - T_l), \tag{1}$$

where

$$\phi_m(t) = \sum_{q=0}^{Q-1} b_{m,q} e^{j2\pi c_{m,q} \Delta f t} 1_{(0,\Delta t)}(t - q\Delta t),$$

and

$$1_{(0,\Delta t)}(t) \triangleq \begin{cases} 1, & \text{if } 0 < t < \Delta t, \\ 0, & \text{otherwise.} \end{cases}$$

$T_l$ and $\Delta t$ denote the pulse repetition interval and hopping interval duration, respectively, and $q$ and $Q$ represent the hopping index and the length of the code, respectively. The duration of the pulse is $T_\phi = Q\Delta t$, and the bandwidth of the pulses is approximately $K\Delta f$. We assume $\Delta f \Delta t = 1$. The frequencies $c_{m,q}$ of the transmitted signal during each hopping interval and the amplitudes $b_{m,q}$ of the transmitted sinusoid are the waveform design parameters. The optimal design of the frequency hopping waveform amounts to choosing $c_{m,q}$ and $b_{m,q}$ for all the transmitters and all the hopping intervals. We assume each $c_{m,q} \in \{1, \ldots, K\}$, where $K$ is a positive integer. Further, to maintain the orthogonality of the waveforms, $c_{m,q}$ satisfies,

$$c_{m,q} \neq c_{m',q}, \quad \text{for } m \neq m',\ \forall q. \tag{2}$$

For amplitudes, we constrain $b_{\min} \leq |b_{m,q}| \leq b_{\max}$ for all transmitters and frequencies. This constraint provides control over the power of the transmitted radar signals.

Further, we normalize the transmitted energy for each waveform by assuming $\sum_{q=0}^{Q-1} |b_{m,q}|^2 = 1$. For convenience, we arrange $c_{m,q}$ into an $M_T \times Q$ dimensional code matrix $\boldsymbol{C} = \{c_{m,q}\}_{M_T \times Q}$, which describes all the transmitted frequencies. Similarly, we arrange $b_{m,q}$ into an $M_T \times Q$ dimensional amplitude matrix $\boldsymbol{B} = [\boldsymbol{b}_1^T; \ldots; \boldsymbol{b}_{M_T}^T]$, where $\boldsymbol{b}_{\mathrm{m}} = [b_{m,1}, \ldots, b_{m,Q}]^T$.

Consider a target at $(\tau, \nu, f)$ where $\tau$ is the delay of the target, $\nu$ is the Doppler frequency, and $f$ is the spatial frequency:

$$f = \frac{d_R \sin(\theta)}{\lambda}, \tag{3}$$

where $\lambda$ is the wavelength of the carrier. We assume that each of the targets contains multiple individual isotropic scatterers. The bandwidth of the transmitted waveform determines the resolution of the system. We require very high bandwidth to resolve each of the individual scatterers of the target. Due to practical bandwidth constraints, however, the system cannot resolve these individual scatters. Therefore, this collection of scatterers can be expressed as one point scatterer that represents the radar cross section (RCS) center of gravity of these multiple scatters [20]. Therefore, each target has a frequency-dependent RCS. The point target assumption has been widely used earlier in the literature for both colocated MIMO radar [3–6] and distributed MIMO radar [2, 21]. Note that our proposed approach based on game theory is also applicable to the extended target case as long as we can formulate corresponding objective functions based on different criteria.

The target response at the $k$th receive antenna is a summation of all reflected signals from all emitters, expressed as

$$y_k(t) = \sum_{m=1}^{M_T} a_{m,q} \bar{u}_m(t-\tau) e^{j2\pi\nu t} e^{j2\pi f(\gamma m + k)} + e_k(t), \tag{4}$$

where

$$\bar{u}_m(t) = \sum_{l=0}^{L-1} \sum_{q=0}^{Q-1} b_{m,q} e^{j2\pi c_{m,q} \Delta f (t - T_l)} 1_{(0,\Delta t)}(t - q\Delta t - T_l). \tag{5}$$

Here, $\gamma \triangleq d_T/d_R$, $a_{m,q}$ represents the target's RCS and $e_k(t)$ is the additive noise received at the $k$th receiver, assumed to follow Gaussian distribution. Equation (4) gives the measurement model for one target.

Now, we consider the situation of multiple targets. We assume that there are $R$ targets in the illuminated region. Based on the assumption that all the targets are far located from the antennas, the angle $\theta$ is assumed to be the same. Therefore, the spatial frequency is independent of targets. Therefore, the received signal, which is a summation of the reflected signals from all the targets, can be expressed as

$$y_k(t) = \sum_{m=1}^{M_T} \sum_{r=1}^{R} a_{m,q}^r \bar{u}_m(t - \tau^r) e^{j2\pi\nu^r t} e^{j2\pi f(\gamma m + k)} + e_k(t). \tag{6}$$

Note that the delay and Doppler are all target dependent in the multiple targets case. Besides, the RCS will also be target dependent, expressed as $a_{m,q}^r$. After sampling the received signal, we obtain

$$\begin{aligned} y_k(n) = &\sum_{m=1}^{M_T} \sum_{r=1}^{R} \sum_{l=0}^{L-1} \sum_{q=0}^{Q-1} a_{m,q}^r b_{m,q} e^{j2\pi c_{m,q} \Delta f (nT_S - T_l - \tau^r)} \\ &\times 1_{(0,\Delta t)}(nT_S - q\Delta t - T_l - \tau^r) e^{j2\pi\nu^r nT_S} \\ &\times e^{j2\pi f(\gamma m + k)} + e_k(n), \end{aligned}$$

$\forall n = 1, \ldots, N$, where $N$ is the total number of samples at each receiver during one processing interval and $T_S$ denotes the corresponding sampling interval.

## B. Sparse Model

Sparsity-based approaches have been broadly used for signal processing in the radar field [19, 22–25]. Suppose we discretize the delay and Doppler space into $D$ and $W$ uniformly separated grid points. Generally, the values of $D$ and $W$ can be very large. For convenience, we restrict their values to be smaller numbers by restricting our interested region to a narrow one. Therefore, we have a total of $DW$ number of grid points, among which only $R$ correspond to the real targets. Let $\tau^d$ and $\nu^w$ represent the delay and Doppler of the grid point. For each grid point, we define the basis function as

$$\begin{aligned} &\tilde{\psi}_{m,k,q}(n, d, w) \\ &\quad = \sum_{l=0}^{L-1} e^{j2\pi c_{m,q} \Delta f (nT_S - T_l - \tau^d)} \\ &\qquad \times 1_{0,\Delta t}(nT_S - q\Delta t - T_l - \tau^d) e^{j2\pi\nu^w nT_S} e^{j2\pi f(\gamma m + k)}. \end{aligned}$$

Stacking the basis function according to samples, we obtain an $N \times 1$ vector

$$\tilde{\psi}_{m,k,q}(d, w) = [\tilde{\psi}_{m,k,q}(1, d, w), \ldots, \tilde{\psi}_{m,k,q}(N, d, w)]^T.$$

Then we stack $\psi_{m,k,q}(d, w)$ with respect to receivers into an $NM_R \times 1$ vector

$$\tilde{\psi}_{m,q}(d, w) = [\tilde{\psi}_{m,1,q}(d, w)^T, \ldots, \tilde{\psi}_{m,M_R,q}(d, w)^T]^T.$$

Now, each $\tilde{\psi}_{m,q}(d, w)$ is the basis vector for a different transmitter and frequency. For all transmitters and frequencies, we further stack $\tilde{\psi}_{m,q}(d, w)$ into an $NM_R \times M_T Q$ matrix

$$\boldsymbol{\Psi}(d, w) = [\tilde{\psi}_{1,1}(d, w), \ldots, \tilde{\psi}_{1,Q}(d, w), \ldots, \tilde{\psi}_{M_T,Q}(d, w)].$$

Considering all the combination of $(d_i, w_j), i = 1, \ldots, D, j = 1, \ldots, W$, we can finally stack $\boldsymbol{\Psi}(d, w)$ into an $NM_R \times DWM_TQ$ matrix

$$\boldsymbol{\Psi} = [\boldsymbol{\Psi}(d_1, w_1), \ldots, \boldsymbol{\Psi}(d_1, w_W), \ldots, \boldsymbol{\Psi}(d_D, w_W)]. \tag{7}$$

Equation (7) is the dictionary matrix, defining the basis elements of the sparse representation. Considering all the different transmitters and frequency intervals, we stack $a_{m,q}^r b_{m,q}$ into an $M_TQ$ vector

$$\boldsymbol{x}^r = [a_{1,1}^r b_{1,1}, \ldots, a_{1,Q}^r b_{1,Q}, \ldots, a_{M_T,Q}^r b_{M_T,Q}]^T.$$

Now, we define the sparse vector as

$$\boldsymbol{x}(d, w) = \begin{cases} \boldsymbol{x}^r, & \text{if } (\tau^d, \nu^w) = (\tau^r, \nu^r), \\ \boldsymbol{0}, & \text{otherwise.} \end{cases}$$

Further, we stack the vectors $\boldsymbol{x}(d, w)$ corresponding to different delay and Doppler grid points to obtain a $DWM_TQ$ dimensional block-sparse vector

$$\boldsymbol{x} = [\boldsymbol{x}(1, 1)^T, \ldots, \boldsymbol{x}(d, w)^T, \ldots, \boldsymbol{x}(D, W)^T]^T.$$

In this vector, there are only $R$ nonzero blocks, corresponding to different targets. Additionally, we stack the measurements and noise samples at all receivers to obtain the measurement model

$$\boldsymbol{y} = \boldsymbol{\Psi}\boldsymbol{x} + \boldsymbol{e}, \tag{8}$$

where $\boldsymbol{y} = [\boldsymbol{y}_1^T, \boldsymbol{y}_2^T, \ldots, \boldsymbol{y}_{M_R}^T]^T$, an $NM_R \times 1$ vector; $\boldsymbol{y}_k = [\boldsymbol{y}_k(1), \boldsymbol{y}_k(2), \ldots, \boldsymbol{y}_k(N)]^T$, an $N \times 1$ vector; $\boldsymbol{e} = [\boldsymbol{e}_1^T, \boldsymbol{e}_2^T, \ldots, \boldsymbol{e}_{M_R}^T]^T$, an $NM_R \times 1$ vector; and $\boldsymbol{e}_k = [\boldsymbol{e}_k(1), \boldsymbol{e}_k(2), \ldots, \boldsymbol{e}_k(N)]^T$, an $N \times 1$ vector. Owing to the orthogonality of the waveforms, block-matching pursuit (BMP) [26] is suitable for our problem. We will use the BMP method to recover the unknown target parameters from the measurements.

## III. JOINTLY OPTIMAL DESIGN USING GAME THEORY

Researchers have studied and optimally designed the amplitudes and frequency-hopping codes separately, achieving improved performance. In this section, we will present the objective functions for joint design of the frequency-hopping waveforms. The function with amplitudes is based on sparse recovery, whereas the function with frequency-hopping codes is based on the ambiguity function. Then we combine the two objective functions, jointly designing the waveforms using game theory.

### A. Objective Function for Frequency-Hopping Codes

The ambiguity function characterizes the resolution of radar waveforms and has been used as an effective tool to design radar systems. Similarly, we apply the MIMO radar ambiguity function to design the frequency-hopping waveforms.

For frequency-hopping code design [5], to obtain a sharp ambiguity function, we need to design the pulses $\{\phi_m(t)\}$ so that the following objective function

$$\Omega(\tau, \bar{f}, \bar{f}') \triangleq \sum_{m=0}^{M_T-1} \sum_{m'=0}^{M_T-1} r^{\phi}_{m,m'}(\tau) e^{j2\pi(\bar{f}m - \bar{f}'m')\gamma} \tag{9}$$

is sharp around the line $\{(\tau, \bar{f}, \bar{f}')|\tau = 0, \bar{f} = \bar{f}'\}$, where $\bar{f}$ and $\bar{f}'$ represent the normalized target's true spatial frequency and the assumed spatial frequency at the receiver, respectively. In (9), the cross-correlation function is defined as

$$\begin{aligned} r^{\phi}_{m,m'}(\tau) &= \sum_{q=0}^{Q-1} \sum_{q'=0}^{Q-1} b_{m,q} b_{m',q'} \chi^{\text{rect}}(\tau - (q' - q)\Delta t, (c_{m,q} - c_{m',q'})\Delta f) \\ &\quad \times e^{j2\pi \Delta f((c_{m,q} - c_{m',q'}))q\Delta t} e^{j2\pi \Delta f c_{m',q'}\tau}, \end{aligned}$$

with $\chi^{\text{rect}}(\tau, \nu)$ being the single input/multiple output ambiguity function of the rectangular pulse $s(t)$, given by

$$\chi^{\text{rect}}(\tau, \nu) \triangleq \int_0^{\Delta t} s(t)s(t + \tau)e^{j2\pi\tau} dt.$$

However, to achieve good system resolution, we need to eliminate the other peaks in $\Omega(\tau, \bar{f}, \bar{f}')$ not on the line $\{(\tau, \bar{f}, \bar{f}')|\tau = 0, \bar{f} = \bar{f}'\}$. We solve this by adding penalties on these peaks, forcing the energy to be evenly spread over the delay and spatial frequency spaces. One way to achieve this goal is to minimize the $p$-norm of $\Omega(\tau, \bar{f}, \bar{f}')$. The resulting optimization problem is

$$\begin{aligned} \min_{\boldsymbol{C}} \quad & \int_{-\infty}^{\infty} \int_0^1 \int_0^1 |\Omega(\tau, \bar{f}, \bar{f}')|^p d\bar{f} d\bar{f}' d\tau, \\ \text{subject to} \quad & c_{m,q} \in \{0, 1, \ldots, K - 1\}, \\ & c_{m,q} \neq c_{m',q}, \text{ for } m \neq m', \end{aligned}$$

When we consider the sparse recovery model, the delay range is $[0, \tau^D]$. Therefore, the optimization problem can be reduced to

$$\min_{\boldsymbol{C}} f_p(\boldsymbol{B}, \boldsymbol{C}) = \int_0^{\tau^D} \int_0^1 \int_0^1 |\Omega(\tau, \bar{f}, \bar{f}')|^p d\bar{f} d\bar{f}' d\tau. \tag{10}$$

### B. Objective Function for Amplitudes

BMP is a sparse recovery method for signals that exhibit block sparse structure, and we will use the BMP method to estimate the target RCS, adaptively designing the amplitudes of frequency-hopping waveforms [6].

Recall that the nonzero element of the sparse vector $\boldsymbol{x}$ is the product of $a^r_{m,q}$ and $b_{m,q}$, and the design parameters are $b_{m,q}$. During the initialization step, we set $b_{m,q} = 1$. Therefore, the nonzero entries of the sparse vector $\boldsymbol{x}$ depend only on the attenuation $a^r_{m,q}$. Hence, we obtain $\hat{a}^r_{m,q}$ as the estimates of the target attenuations after sparse support recovery. We use $\hat{a}^r_{m,q}$ to replace $a^r_{m,q}$ in the following design problem. In practice, provided enough measurements and high signal-to-noise-ratio (SNR), we expect to achieve the estimation of $\hat{a}^r_{m,q}$ with high accuracy. We define $\hat{x}^r_m$ to be the summation of the energies of the estimates for target $r$ and transmitter $m$

$$\hat{x}^r_m = \sum_{q=0}^{Q-1} b^2_{m,q} |\hat{a}^r_{m,q}|^2.$$

Then we have the vector $\tilde{\boldsymbol{x}}_m(\boldsymbol{b}_m) = [\hat{x}^1_m(\boldsymbol{b}_m), \ldots, \hat{x}^R_m(\boldsymbol{b}_m)]$. With the goal of estimating all the $R$ targets, we want to maximize the smallest recovered estimate. We propose to use the following two optimization strategies.

1) We maximize the smallest recovered estimate in $\tilde{\boldsymbol{x}}_m(\boldsymbol{b}_m)$ for each transmitter. Therefore, we have $M_T$ optimization problems corresponding to $M_T$ transmitters. They are independent of each other, with separate constraints. We denote this strategy as ADS constraints. The optimization problem for transmitter $m$ is

$$\begin{aligned} &\max_{\boldsymbol{b}_m} \quad \min_{r\in 1,\dots,R}\{\tilde{x}_m^r(\boldsymbol{b}_m)\}, \\ &\text{subject to} \quad |b_{m,q}| \geq b_{\min},\ |b_{m,q}| \leq b_{\max}, \\ &\qquad \sum_{q=0}^{Q-1} |b_{m,q}|^2 = 1. \end{aligned} \tag{11}$$

The objective of (11) is equivalent to

$$\min_{\boldsymbol{b}_m} \ \tilde{f}_m(\boldsymbol{b}_m, \boldsymbol{C}) = \max_{r\in 1,\dots,R}\{Z - \tilde{x}_m^r(\boldsymbol{b}_m)\}, \tag{12}$$

where $Z$ is a large constant, guaranteeing that $Z - \tilde{x}_m^r(\boldsymbol{b}_m)$ is nonnegative.

2) We maximize the smallest recovered estimate, obtained by fusing all the $M_T$ transmitters. Considering that different transmitters may have different energies, we use a sum of the transmitted energy constraint across all $M_T$ transmitters. We denote this strategy as ADF all transmitters. The optimization problem is

$$\begin{aligned} &\max_{\boldsymbol{B}} \quad \min_{r\in 1,\dots,R}\left\{\sum_{m=1}^{M_T} \tilde{x}_m^r(\boldsymbol{b}_m)\right\}, \\ &\text{subject to} \quad |b_{m,q}| \geq b_{\min},\ |b_{m,q}| \leq b_{\max}, \\ &\qquad \sum_{m=1}^{M_T}\sum_{q=0}^{Q-1} |b_{m,q}|^2 = 3. \end{aligned} \tag{13}$$

Note that the energy constraint is 3, making the summation of energy the same as with ADS. Similar to ADS, we get the equivalent form:

$$\min_{\boldsymbol{B}} \ \tilde{f}(\boldsymbol{B}, \boldsymbol{C}) = \max_{r\in 1,\dots,R}\left\{Z - \sum_{m=1}^{M_T} \tilde{x}_m^r(\boldsymbol{b}_m)\right\}. \tag{14}$$

## C. Game Model

A normal strategic game is a model of interacting decision makers, consisting of players, their strategies, and the players' cost functions [27]. Each player chooses one strategy from his corresponding set of possible strategies. The goal of the players is to choose strategies that minimize their own cost functions.

If we consider ADS, then in our joint design problem we have $M_T + 1$ objective functions. As for the $M_T$ objective functions for amplitude design, their variable choices are independent of each other. It means that the choice of any $\boldsymbol{b}_i$ is irrelevant to the choice of $\boldsymbol{b}_j$ for $i \neq j$. Accordingly, we write these $M_T$ cost functions into one summation function:

$$f_s(\boldsymbol{B}, \boldsymbol{C}) = \sum_{m=1}^{M_T} \tilde{f}_m(\boldsymbol{b}_m, \boldsymbol{C}). \tag{15}$$

Therefore, the optimization problem (12) is equivalent to

$$\min_{\boldsymbol{B}} \ f_s(\boldsymbol{B}, \boldsymbol{C}). \tag{16}$$

Now, we have two objective functions, $f_s(\boldsymbol{B}, \boldsymbol{C})$ corresponding to amplitude design and $f_p(\boldsymbol{B}, \boldsymbol{C})$ corresponding to code design. We assume that each player is associated with one objective function. Therefore, we have two players. The cost function for the first player is chosen as

$$f_1(\boldsymbol{B}, \boldsymbol{C}) = f_p(\boldsymbol{B}, \boldsymbol{C}). \tag{17}$$

The cost function for the second player is

$$f_2(\boldsymbol{B}, \boldsymbol{C}) = f_s(\boldsymbol{B}, \boldsymbol{C}). \tag{18}$$

$(\boldsymbol{B}, \boldsymbol{C})$ are the design variables. The first player wants to choose parameters $\boldsymbol{C}$ that minimize his or her cost function $f_1(\boldsymbol{B}, \boldsymbol{C})$, and similarly the second player wants to find variables $\boldsymbol{B}$ to minimize his or her own cost function $f_2(\boldsymbol{B}, \boldsymbol{C})$. The strategy spaces for the two players are respectively

$$\begin{aligned} \mathcal{B} = \{\boldsymbol{B} \,|\, &|b_{m,q}| \geq b_{\min}, |b_{m,q}| \leq b_{\max}, \\ &\sum_{q=0}^{Q-1} |b_{m,q}|^2 = 1, m = 1, \dots, M_T\}, \end{aligned}$$

and

$$\mathcal{C} = \{C | c_{m,q} \in \{1,\ 2, \dots, K\}^{M_T Q}, c_{m,q} \neq c_{m',q}, \text{for } m \neq m'\}.$$

If we consider ADF, then in our joint design problem we have two objective functions. The differences in the case of ADS are the second player's cost function and its strategy space:

$$f_1(\boldsymbol{B}, \boldsymbol{C}) = \tilde{f}(\boldsymbol{B}, \boldsymbol{C}), \tag{19}$$

with

$$\mathcal{B} = \{\boldsymbol{B} \,|\, |b_{m,q}| \geq b_{\min}, |b_{m,q}| \leq b_{\max}, \sum_{m=1}^{M_T}\sum_{q=0}^{Q-1} |b_{m,q}|^2 = 3\}.$$

$(\boldsymbol{B}, \boldsymbol{C})$ denotes a profile of actions by the two players. A Nash equilibrium is a profile of strategies such that the strategy for each player is an optimal response to the strategy of the other players. Supposing $(\boldsymbol{B}^*, \boldsymbol{C}^*)$ is a Nash equilibrium for this game, then it should satisfy

$$f_1(\boldsymbol{B}^*, \boldsymbol{C}^*) \leq f_1(\boldsymbol{B}, \boldsymbol{C}^*), \quad \forall \boldsymbol{B} \in \mathcal{B},$$

and

$$f_2(\boldsymbol{B}^*, \boldsymbol{C}^*) \leq f_2(\boldsymbol{B}^*, \boldsymbol{C}), \quad \forall \boldsymbol{C} \in \mathcal{C}.$$

The feasible space $\mathcal{C}$ for player 2 is discrete. Owing to the numerous choices of $\boldsymbol{C}$, up to $K^{M_T Q}$, it is almost impossible for us to find the global minimal point for the cost function $f_1$, making it difficult to find the Nash equilibrium. For this optimization problem, we prefer to use the simulated annealing algorithm, which is quite suitable [17]. One problem is that the feasible space for the code matrix is extremely large. Nevertheless simulated annealing achieves an acceptable solution, yielding a good approximation to the global optimum, the $\epsilon$-AE [18].

DEFINITION 1 *Let $G = (N, \boldsymbol{A}, \boldsymbol{f} : \boldsymbol{A} \rightarrow \mathbb{R}^N)$ be an N-player game with action sets $\boldsymbol{A} = \boldsymbol{A}_1 \times \ldots \times \boldsymbol{A}_N$ and cost functions $\boldsymbol{f} = [\boldsymbol{f}_1, \ldots, \boldsymbol{f}_N]^T$. Suppose $\epsilon$ is a nonnegative parameter, a strategy vector $(a_1^*, \ldots, a_N^*) \in \boldsymbol{A}$ is an $\epsilon$-AE for G if*

$$f_i(a_1^*, \ldots, a_N^*) \leq f_i(a_1^*, \ldots, a_{i-1}^*, a_i, a_{i+1}^*, \ldots, a_N^*) + \epsilon,$$
$$\forall a_i \in \boldsymbol{A}_i, \ \ i \in N.$$

Our definition here is the $\epsilon$-AE in a pure strategy game, which is a different definition from that used in most of the literature for a mixed strategy game. In our problem, we will focus on finding the $\epsilon$-AE for the proposed game.

### D. Optimization Algorithm Using Game Theory

1) *Noncooperative Case*: First, we consider the noncooperative case, with each player having no knowledge of the other players' information. They know only their own information. The algorithm is expressed as follows:

Initialize $\boldsymbol{C}_0$ randomly from feasible space $C$, and initialize $\boldsymbol{b}_{m0}$, $m = 1, \ldots, M_T$ for ADS or initialize $\boldsymbol{B}$ for ADF, whose elements are set to be equal.
At step $k$, fix $\boldsymbol{C}_k$, then conduct the single objective optimization design for player 2:

$$\min_{\boldsymbol{B}} \ f_2(\boldsymbol{B}, \boldsymbol{C}_k),$$

resulting in the optimized $\boldsymbol{B}_{k+1}$. Using the newly generated $\boldsymbol{B}_{k+1}$, we optimize player 1's objective function

$$\min_{\boldsymbol{C}} \ f_1(\boldsymbol{B}_{k+1}, \boldsymbol{C}),$$

obtaining $\boldsymbol{C}_{k+1}$.
Replace $\boldsymbol{B}_k, \boldsymbol{C}_k$ with $\boldsymbol{B}_{k+1}, \boldsymbol{C}_{k+1}$ and repeat the above step until an $\epsilon$-AE is satisfied or $k$ is large enough.

We apply the convex programming software CVX [28, 29] to solve the single amplitude optimization problem. The simulated annealing algorithm solves the code optimization problem, which has a large discrete feasible set.

The convergence of the proposed optimization algorithm is an important issue. However, the cost functions (10), (12), and (14) in our problem are rather complex. Besides, the size of the discrete feasible space for code matrix will be extremely large as $M_T$ or $K$ increases. Both of these two reasons make it difficult for us to analytically prove the convergence, which, however, is shown through numerical examples in Section IV. Nevertheless, we would like to add the following remarks regarding the convergence issue.

REMARKS First, we define four notations, two at a time:

$$f_{1C}^k = f_1(\boldsymbol{B}_{k-1}, \boldsymbol{C}_k) \tag{20}$$

$$f_{2C}^k = f_2(\boldsymbol{B}_{k-1}, \boldsymbol{C}_k). \tag{21}$$

These are the first and second cost functions at step $k$ after designing only $\boldsymbol{C}$, using the former amplitude strategy $\boldsymbol{B}_{k-1}$ of step $k-1$ and the newly obtained code strategy $\boldsymbol{C}_k$. Now we define

$$f_{1B}^k = f_1(\boldsymbol{B}_k, \boldsymbol{C}_k) \tag{22}$$

$$f_{2B}^k = f_2(\boldsymbol{B}_k, \boldsymbol{C}_k). \tag{23}$$

These are the first and second cost functions at step $k$ after designing both $\boldsymbol{C}$ and $\boldsymbol{B}$, using the newly obtained $\boldsymbol{B}_k$ and $\boldsymbol{C}_k$. Considering the first player $f_1$, due to the conflict between these two players, we expect that $f_{1C}^k$ would decrease compared to $f_{1B}^{k-1}$ and that $f_{1B}^k$ would increase compared to $f_{1C}^k$. Note that the increase and decrease are not strict. Namely, there is some variation, and this is explainable from a game theory point of view. Therefore, if convergence exists, these two cost functions $f_{1C}^k$ and $f_{1B}^k$ should cross with each other somewhere after a number of iterations. We define this crossing point as the convergence point with $f_{1C}^k = f_{1B}^{k-1}$, which means the code matrix does not change at step $k$. Using the same code matrix, the minimization process for the second player would not change, resulting in the same amplitude matrix. This is exactly what convergence means. Thus, in the algorithm, one stop criterion is chosen as $f_{1C}^k = f_{1B}^{k-1}$. It is the same case with the second player. We will show the convergence performance through numerical examples.

Second, our algorithms converge to different points with respect to different trials. Namely, the convergence points are not fixed. This is reasonable because the code space is extremely large; thus, we cannot find a global optimal solution for the first player, namely $f_1$. We reduce the original big problem into a smaller problem, achieving lower complexity at the price of solution optimality. However, we want to emphasize that the obtained convergence points perform sufficiently well, especially when we conduct target estimation. We will verify this through numerical examples in Section IV.

Third, all the obtained convergence points satisfy the AE conditions in Definition 1.

PROOF Following the discussion in the first item, we denote the convergence point as $f_1(\boldsymbol{B}^*, \boldsymbol{C}^*)$ and $f_2(\boldsymbol{B}^*, \boldsymbol{C}^*)$. On the other hand, suppose that the global optimal point of player 1 with fixed $\boldsymbol{B}^*$ is $\boldsymbol{C}^{**}$. If we let

$$\epsilon = f_1(\boldsymbol{B}^*, \boldsymbol{C}^*) - f_1(\boldsymbol{B}^*, \boldsymbol{C}^{**}), \tag{24}$$

we can obtain

$$f_1(\boldsymbol{B}^*, \boldsymbol{C}^*) \leq f_1(\boldsymbol{B}^*, \boldsymbol{C}) + \epsilon. \tag{25}$$

For player 2, $f_2(\boldsymbol{B}^*, \boldsymbol{C}^*)$ is the global minimal point for $f_2(\boldsymbol{B}, \boldsymbol{C}^*)$ with fixed $\boldsymbol{C}^*$. Thus we have

$$f_2(\boldsymbol{B}^*, \boldsymbol{C}^*) \leq f_2(\boldsymbol{B}, \boldsymbol{C}^*) \leq f_2(\boldsymbol{B}, \boldsymbol{C}^*) + \epsilon. \tag{26}$$

Equations (6) and (7) are exactly the conditions for $(\boldsymbol{B}^*, \boldsymbol{C}^*)$ to be an $\epsilon$-AE in Definition 1.

2) *Cooperative Case*: In the cooperative[1] case, we suppose each player knows part of the other players' information by incorporating their cost functions in his or her own cost function. The resulting cost function for each player is

$$f_i^* = w_{i,i} f_i + \sum_{j \neq i} w_{i,j} f_j, \tag{27}$$

where $\sum_j w_{i,j} = 1$, $w_{i,j} = w_{j,i}$. In our problem, we choose the second player's cost function to remain the same, without considering the first player's influence. All that changes is the first player's objective function. Additionally, we replace the absolute cost function with a relative cost function. Details are shown as follows:

---

Initialize $\boldsymbol{C}_0$ randomly from feasible space $\mathcal{C}$, and initialize $\boldsymbol{b}_{m0}, m = 1, \ldots, M_T$ for ADS or initialize $\boldsymbol{B}$ for ADF, whose elements are set to be equal.

At step $k$, fix $\boldsymbol{C}_k$, then conduct the single objective optimization design for player 2:

$$\min_{\boldsymbol{B}} \ f_2(\boldsymbol{B}, \boldsymbol{C}_k),$$

resulting in the optimized $\boldsymbol{B}_{k+1}$. Using the newly generated $\boldsymbol{B}_{k+1}$, we optimize player 1's new objective function

$$\begin{aligned} \min_{\boldsymbol{C}} \ f_1^* = &\sum_{m=1}^{M_T} w_m \frac{\tilde{f}_m(\boldsymbol{b}_{m,k+1}, \boldsymbol{C})}{\tilde{f}_m(\boldsymbol{b}_{m,k}, \boldsymbol{C}_k)} \\ &+ w_{M_T+1} \frac{f_1(\boldsymbol{B}_{k+1}, \boldsymbol{C})}{f_1(\boldsymbol{B}_k, \boldsymbol{C}_k)}, \end{aligned}$$

obtaining $\boldsymbol{C}_{k+1}$.

Replace $\boldsymbol{B}_k, \boldsymbol{C}_k$ with $\boldsymbol{B}_{k+1}, \boldsymbol{C}_{k+1}$ and repeat the above step until an $\epsilon$-AE is satisfied or $k$ is large enough.

---

The convergence analysis for the cooperative case is similar to that of the noncooperative case.

## IV. NUMERICAL SIMULATIONS

In this section, we use numerical examples to demonstrate the performance improvement obtained by joint design using game theory. We consider a uniform linear transmitting array with transmitter and receiver numbers $M_T = 3$ and $M_R = 3$, respectively. Choose $\theta = 30^\circ$ and let the array spacing $d_T = d_R = \frac{\lambda}{2}$. The length of the frequency-hopping code $Q$ equals 5. The number of frequencies $K$ equals 7. Suppose $L = 10$ pulses comprise a waveform. The chip duration is $\Delta t = 1\ \mu$s, whereas the time interval between pulses is 3 ms. The minimum hopping frequency interval is $\Delta f = 1$ MHz. Because we chose $K = 7$, the maximum hopping-frequency is $K\Delta f = 7$ MHz. Therefore, we sample at a Nyquist rate of $14 \times 10^6$ samples/s. Further, we suppose three targets are present in the scenario. We specify the amplitudes of $K$ attenuations for each target

$$\begin{aligned} \boldsymbol{a}^1 &= [0.4, 0.2, 0.5, 0.8, 0.1, 0.4, 0.3], \\ \boldsymbol{a}^2 &= [0.6, 0.2, 0.8, 0.9, 0.1, 0.3, 0.5], \\ \boldsymbol{a}^3 &= [0.2, 0.4, 0.3, 0.7, 0.4, 0.1, 0.9]. \end{aligned}$$

We can use this attenuation information to estimate the RCS corresponding to different hopping-frequencies and transmitters.

When considering sparse recovery, we discretize the target delay-Doppler space. The grid size in delay is $\Delta t = 1\ \mu$s, and the Doppler dimension is 10 Hz. The delay space is uniformly divided in the interval $[0, 10]\ \mu$s, and the Doppler grid points lie uniformly in the interval [0, 100] Hz. Therefore, we have a total of $V = 11 \times 11 = 121$ grid points, out of which only three correspond to the true targets. We assume the true delays and Doppler shifts of the targets are

$$\begin{aligned} &\left[\tau^1, \tau^2, \tau^3\right] = [4, 9, 1]\ \mu s, \text{ and} \\ &\left[\nu^1, \nu^2, \nu^3\right] = [80, 60, 40] \text{ Hz}. \end{aligned}$$

Note that we assume we know the approximate target locations, namely within the delay interval [0,10] $\mu$s and Doppler interval [0, 100] Hz. When we consider a real problem with a large surveillance region, this approximate knowledge of the target information can be obtained by conducting target detection beforehand or by using a coarse grid first [30]. We define the SNR as

$$\text{SNR} = 10 \log \left( \frac{\|\Psi \boldsymbol{x}\|^2}{\text{E}(\|e\|^2)} \right) \text{dB},$$

where $\text{E}\{\cdot\}$ denotes the expected value of $\{\cdot\}$.

In the following numerical examples, we investigate the performance of noncooperative joint design with ADS (NC-ADS) and cooperative joint design with ADS (C-ADS) in sub-Sections IVA–IVC. Then, in sub-Section IVD, we compare the performance of joint design employing ADS with those employing ADF (NC-ADF and C-ADF). The convergence issue is investigated in sub-Section IVE.

### A. Frequency-Hopping Code Design

We compare the performance of the proposed design method and the existing separate design methods using the empirical cumulative distribution function (CDF) of $|\Omega(\tau, f, f')|$ applied in [5]. We use the Monte Carlo method by sampling from the function $|\Omega(\tau, f, f')|$, and plot the percentage of samples of $|\Omega(\tau, f, f')|$ less than different magnitudes. Thus, the larger the CDF for a specific magnitude, the fewer undesired peaks the waveform yields, and the better the waveform performs. We have normalized the greatest value to 0 dB.

[1] The cooperative case here has a different definition from cooperative game. We consider the coalition between different players.

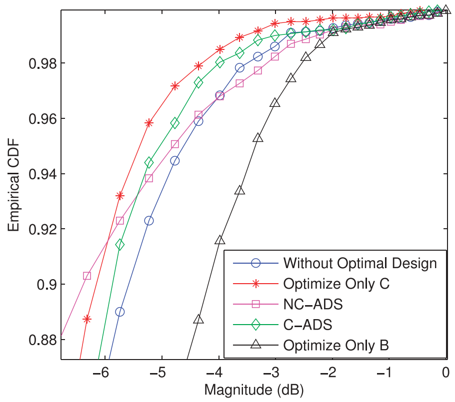


Fig. 1. Empirical CDF of $|\Omega(\tau, f, f')|$ for five different design methods.

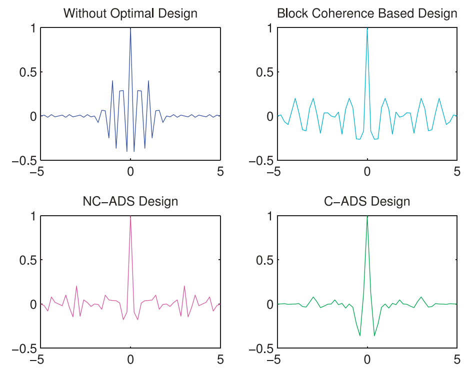


Fig. 2. Cross-correlation function $r^{\phi}_{m,m'}(\tau)$, with $m = m' = 1$, of waveforms generated by proposed methods and one using the block coherence measure. Abscissa axis is delay $(\tau/\Delta t)$, and vertical axis is cross-correlation value.

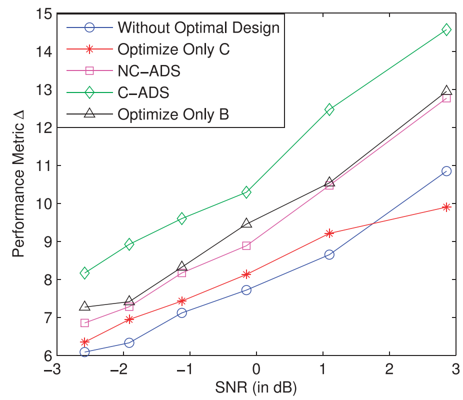


Fig. 3. Performance metric $\Delta$ comparison of five different design methods.

Fig. 1 shows the results of five different design methods: without optimal design, optimize only $\boldsymbol{C}$, NC-ADS, C-ADS, and optimize only $\boldsymbol{B}$. Because the CDF criterion is mainly designed to measure the performance improvement resulting from designing code matrix $\boldsymbol{C}$, it is not surprising to see that the method designing only $\boldsymbol{C}$ achieves the best performance. When designing $\boldsymbol{B}$ only, the performance becomes worse than even the case without any optimal design. This is explainable from a game theory point of view. Each player tries to choose strategies that minimize his or her own cost function, which will not necessarily contribute to the other players' benefits. In this example, it degrades the other players' performance. Game theory-based joint design performs much better than that designing only $\boldsymbol{B}$. Owing to the degraded performance caused by designing $\boldsymbol{B}$, the joint design performs a little worse than that designing only $\boldsymbol{C}$. Note that the C-ADS performs better than the NC-ADS and comes closest to the case of designing $\boldsymbol{C}$ only.

To show the relative superiority of our design methods, we also compare the cross-correlation function of the waveforms generated by the proposed methods with the one designed based on block coherence [6]. We wish to obtain small sidelobes.

From Fig. 2, it is quite evident that the joint design methods, both NC-ADS and C-ADS result in a much better cross-correlation function. The low sidelobes of the cross-correlation function corresponding to the joint design methods are much smaller than those of the counterparts of the waveform designed using block coherence. The reason for the superiority of the joint design methods is because these designs consider eliminating irrelevant peaks of $|\Omega(\tau, f, f')|$, which is highly related to the correlation function.

## B. Amplitude Design

We use the performance metric:

$$\Delta = \frac{\min \hat{\boldsymbol{x}}_S}{\max \hat{\boldsymbol{x}}_{\bar{S}}},$$

where $S$ and $\bar{S}$ denote the recovered support sets of the correct and incorrect target indices, respectively. The numerator and denominator of $\Delta$ denote the weakest target reconstruction and the strongest reconstruction of the incorrect target indices, respectively. Therefore, $\Delta > 1$ guarantees that the correct target indices dominate the others, providing a measure of the recovery accuracy. We want this metric to be as large as possible.

Fig. 3 shows the resulting performance metrics over various SNR using different design methods. Because the performance metric is mainly applied to measure the performance improvement resulting by designing amplitude matrix $\boldsymbol{B}$, similar to what we mentioned earlier, it is not surprising to see that the method designing only $\boldsymbol{B}$ achieves relatively good performance. When designing $\boldsymbol{C}$ only, at some specific SNR, the performance becomes even worse than the case without optimal design. This is also explainable from a game theory point of view. Game theory-based joint design performs much better than one designing only $\boldsymbol{C}$. Owing to the degraded performance caused by designing $\boldsymbol{C}$, the NC-ADS performs a little worse than designing only $\boldsymbol{B}$. However, the C-ADS achieves the best performance, better even than the result from designing $\boldsymbol{B}$ only. This superiority is achieved by cooperating between the players, sharing each other's information about cost functions.

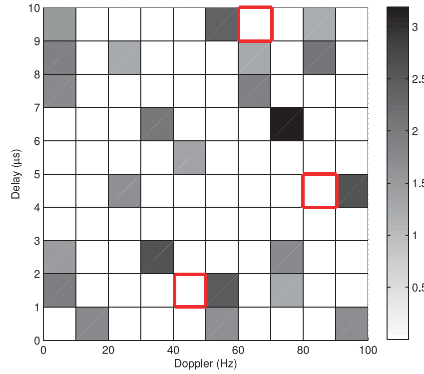


Fig. 4. Target estimates at SNR of –21.58 dB by designing only $\boldsymbol{C}$.

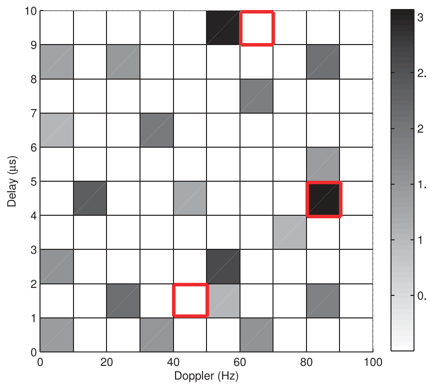


Fig. 5. Target estimates at SNR of –21.58 dB by designing only $\boldsymbol{B}$.

## C. Sparse Support Recovery

As we assumed, three targets are present in the illuminated space. We used 30 iterations for the BMP algorithm. We have assumed the targets will lie exactly on the grid points. However, in reality they may lie in between two grid points, which can be a result of the grid size not being small enough. When such modeling errors occur, the authors in [21] have demonstrated that the reconstruction algorithm BMP will map the estimates to the grid point that is closest to the true target parameter. The same holds for the results in this paper because we are using BMP. The reconstructed target parameters at an SNR of –21.58 dB are shown in Figs. 4–6, corresponding to three different designs. Red squares are the true locations of the three targets. For these two-dimensional plots, the intensity of the grid point corresponds to the specific reconstruction energy.

Fig. 4 shows the performance achieved by designing $\boldsymbol{C}$ only, for which none of the three targets are correctly recovered. Besides, some delay and Doppler are wrongly estimated. For the case designing only $\boldsymbol{B}$, shown in Fig. 5, only one target (4 $\mu$s, 80 Hz) is estimated correctively. However, at the same SNR, our C-ADS joint design based on game theory successfully estimates all three targets, with the three highest intensity points as shown in Fig. 6.

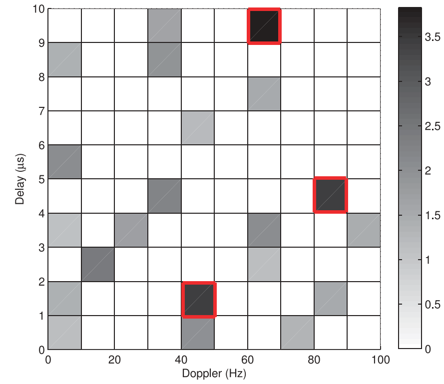


Fig. 6. Target estimates at SNR of –21.58 dB using C-ADS joint design.

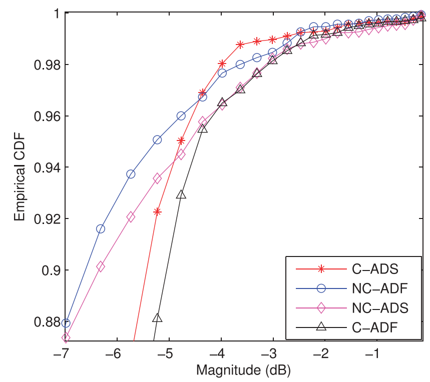


Fig. 7. Empirical CDF of $|\Omega(\tau, f, f')|$ for four joint design methods.

## D. Performance Comparison of ADS and ADF

In the above subsections, we see that the joint design employing ADS shows great advantage over separate designs. In this subsection, we will concentrate on the performance of joint design using ADF and compare its effectiveness with ADS.

First, we consider the performance metric for frequency-hopping codes, as in sub-Section IVA. Fig. 7 shows the results of four joint designs. As for noncooperative designs, ADF outperforms ADS. Namely, the strategy of fusing and constraining all transmitters achieves better performance. We can explain this by considering that, for ADF, different transmitters choose their most suitable energy values based on their respective channel qualities. However, for ADS, all the transmitters are assigned equal energy. As for cooperative design, the fusion strategy loses its superiority: C-ADS performs better than C-ADF. We explain this from the view point of game theory: one player's strategy degrades the other player's performance much more strongly by using ADF than by using ADS.

Next, we consider the performance metric for amplitudes, as in sub-Section IVB. Fig. 8 shows the comparison results, which are exactly the same as those of frequency-hopping codes. In the end, we use sparse support recovery to investigate the estimation performance of the four joint design methods. Just as in sub-Section IVC, three targets are present. The reconstructed target

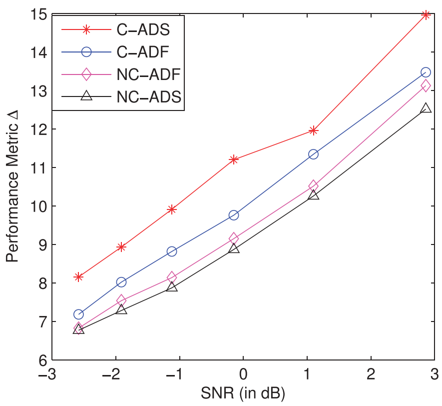


Fig. 8. Performance metric Δ comparison of four joint design methods.

TABLE I
Target Estimates at an SNR of –18.96 dB

| Design Method | $(\tau^1,\ \nu^1)$ | $(\tau^2,\ \nu^2)$ | $(\tau^3,\ \nu^3)$ |
|---|---|---|---|
| NC-ADS | (4 $\mu$s, 70 Hz) | (9 $\mu$s, 60 Hz) | (1 $\mu$s, 40 Hz) |
| NC-ADF | (4 $\mu$s, 80 Hz) | (9 $\mu$s, 60 Hz) | (1 $\mu$s, 40 Hz) |

TABLE II
Target Estimates at an SNR of –20.63 dB

| Design Method | $(\tau^1,\ \nu^1)$ | $(\tau^2,\ \nu^2)$ | $(\tau^3,\ \nu^3)$ |
|---|---|---|---|
| C-ADS | (4 $\mu$s, 80 Hz) | (9 $\mu$s, 60 Hz) | (1 $\mu$s, 40 Hz) |
| C-ADF | (4 $\mu$s, 90 Hz) | (9 $\mu$s, 60 Hz) | (1 $\mu$s, 40 Hz) |

parameters at an SNR of –18.96 dB for NC-ADS and NC-ADF are shown in Table I. We can see that NC-ADF correctly estimates all the three targets, whereas NC-ADS falsely estimates the first target. Table II shows the reconstructed target parameters at an SNR of –20.63 dB for C-ADS and C-ADF. The results show that C-ADS performs better than C-ADF. These results are in accordance with the aforementioned numerical examples.

## E. Convergence

In this subsection, we provide examples to numerically show the convergence of our algorithms. We have made more than 50 trials, and all converge to an $\epsilon$-AE point within $k = 20$ iterations. Note that we consider NC-ADS here, but other algorithms are similar. Figs. 9 and 10 show the convergence performance of both players for nine of these 50 trials. We can see that both players converge after several iterations and reach the $\epsilon$-AE.

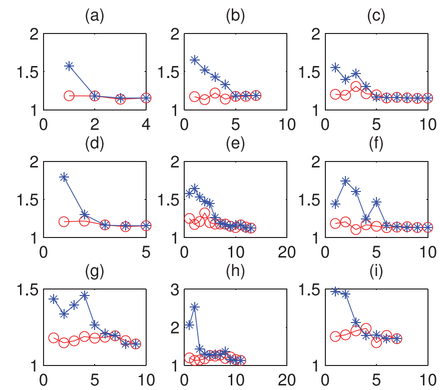

Fig. 9. Convergence performance of player 1 for nine trials using proposed NC-ADS algorithm. Horizontal axis is iteration number $k$, and vertical axis is cost function of first player $f_1$. Blue starred line denotes $f_{1B}$, and red circled line denotes $f_{1C}$.

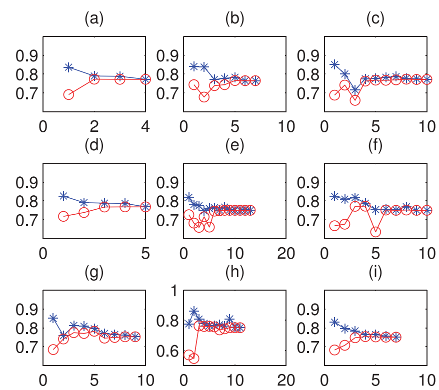

Fig. 10. Convergence performance of player 2 for nine trials using the proposed NC-ADS algorithm. Horizontal axis is iteration number $k$, and vertical axis is cost function of second player $f_2$. Blue starred line denotes $f_{2C}$, and red circled line denotes $f_{2B}$.

# V. CONCLUDING REMARKS

We proposed a joint optimization algorithm using game theory to compute the adaptive code matrix and amplitude matrix for frequency-hopping waveform, which involves both continuous and discrete feasible spaces. For this purpose, we considered a colocated MIMO radar and developed the received signal model and the sparse recovery model. Based on two objective functions derived by using the ambiguity function and sparse recovery, we formulated a game model with two players. For amplitude design, we constructed two effective strategies: ADS constraints and ADF all transmitters. Owing to the large size of the discrete feasible space, we proposed to find an $\epsilon$-AE. Both the cooperative case and noncooperative case were considered to optimize the frequency-hopping codes and amplitudes. We numerically demonstrated the advantage of jointly optimal design methods over separate design methods. We concluded that the optimization algorithm simultaneously chooses frequency-hopping codes that obtain a sharp ambiguity function and amplitudes that increase the possibility of a relatively good target return at the same time. Additionally, we compared the performance of ADS and ADF, showing that ADF outperforms ADS for the noncooperative case. As for the cooperative case, however, ADF is not as good as ADS. In the end, we numerically showed that our algorithms do converge.

In future work, we will develop an efficient algorithm to solve the global equilibrium for large discrete feasible sets, for which we found only an $\epsilon$-AE in this paper. In addition, we will analytically study the convergence of the proposed algorithms. We will also work on other more effective algorithms by incorporating more performance criteria in the constraints to deal with cases where a bad approximate equilibrium exists. For sparse recovery, we will consider nonuniform grid spacing to improve the estimation accuracy and reduce the computational complexity. Future work will also include applications related to real data.

REFERENCES


[1] Li, J., and Stoica, P.
*MIMO Radar Signal Processing*. Hoboken, NJ: Wiley, 2009.

[2] Haimovich, A. M., Blum, R. S., and Cimini, L. J.
MIMO radar with widely separated antennas.
*IEEE Signal Processing Magazine*, **25** (Jan. 2008), 116–129.

[3] Li, J., and Stoica, P.
MIMO radar with colocated antennas.
*IEEE Signal Processing Magazine*, **24** (Sep. 2007), 106–114.

[4] Srinivas, A., Badrinath, S., and Reddy, V. U.
Frequency-hopping code optimization for MIMO radar using the hit-matrix formalism.
In *IEEE Radar Conference*, Washington, D.C., May 2010, 631–636.

[5] Chen, C.-Y., and Vaidyanathan, P.
MIMO radar ambiguity properties and optimization using frequency-hopping waveforms.
*IEEE Transactions on Signal Processing*, **56** (Dec. 2008), 5926–5936.

[6] Gogineni, S., and Nehorai, A.
Frequency-hopping code design for MIMO radar estimation using sparse modeling.
*IEEE Transactions on Signal Processing*, **60** (Jun. 2012), 3022–3035.

[7] Bliss, D. W., and Forsythe, K. W.
Multiple-input multiple-output (MIMO) radar and imaging: Degrees of freedom and resolution.
In *Proceedings of the 37th Asilomar Conf. Signals, Systems, and Computers*, Sardinia, Italy, Nov. 2003, 1057–1064.

[8] Maric, S. V., and Titlebaum, E. L.
A class of frequency hop codes with nearly ideal characteristics for use in multiple-access spread-spectrum communications and radar and sonar systems.
*IEEE Transactions on Communications*, **40** (Sep. 1992), 1442–1447.

[9] Han, K., and Nehorai, A.
Joint frequency-hopping waveform design for MIMO radar estimation using game theory.
Presented at the *Radar Conference (RADAR), 2013 IEEE*, Ottawa, Canada, Apr. 2013.

[10] Marler, R. T., and Arora, J. S.
Survey of multi-objective optimization methods for engineering.
*Structural and Multidisciplinary Optimization*, **26** (Mar. 2004), 369–395.

[11] Schaffer, J. D.
Multiple objective optimization with vector evaluated genetic algorithms.
In *The First International Conference on Genetic Algorithms and Their Applications*, Hillsdale, NJ, 1985, 93–100.

[12] Konak, A., Coit, D. W., and Smith, A. E.
Multi-objective optimization using genetic algorithms: A tutorial.
*Reliability Engineering & System Safety*, **91** (Sep. 2006), 992–1007.

[13] Annamdas, K. K., and Rao, S. S.
Multi-objective optimization of engineering systems using game theory and particle swarm optimization.
*Engineering Optimization*, **41** (Aug. 2009), 737–752.

[14] Rao, S. S.
Game theory approach for multiobjective structural optimization.
*Computers and Structures*, **25** (Apr. 1986), 119–127.

[15] Periaux, J., Chen, H. Q., Mantel, B., Sefrioui, M., and Sui, H. T.
Combining game theory and genetic algorithms with application to DDM-nozzle optimization problems.
*Finite Element in Analysis and Design*, **37** (2001), 417–429.

[16] Wang, J., Wu, Y., and Periaux, J.
Decentralized multi-point optimization algorithms for multi-airfoil design in aerodynamics.
*Journal of Astronautics*, **24** (2003), 71–77.

[17] Kirkpatrick, S., Gelatt, C. D., and Vecchi, M. P.
Optimization by simulated annealing.
*Science*, **220** (1983), 671–680.

[18] Dixon, H.
Approximate Bertrand equilibia in a replicated industry.
*The Review of Economic Studies*, **54** (Jan. 1987), 47–62.

[19] Sen, S., and Nehorai, A.
Sparsity-based multi-target tracking using OFDM radar.
*IEEE Transactions on Signal Processing*, **59** (Apr. 2011), 1902–1906.

[20] Akcakaya, M., Hurtado, M., and Nehorai, A.
MIMO radar detection of targets in compound-Gaussian clutter.
In *2008 42nd Asilomar Conference on Signals, Systems and Computers*, Pacific Grove, CA, Oct. 2008, 26–29.

[21] Gogineni, S., and Nehorai, A.
Target estimation using sparse modeling for distributed MIMO radar.
*IEEE Transactions on Signal Processing*, **59** (Nov. 2011), 5315–5325.

[22] Herman, M., and Strohmer, T.
Compressed sensing radar.
In *Proceedings of the IEEE Radar Conference*, Rome, Italy, May 2008, 1–6.

[23] Baraniuk, R., and Steeghs, P.
Compressive radar imaging.
In *Proceedings of the IEEE Radar Conference*, Boston, Apr. 2007, 128–133.

[24] Chen, C. Y., and Vaidyanathan, P. P.
Compressed sensing in MIMO radar.
In *Proceedings of the 42nd Asilomar Conference on Signal, Systems, Computers*, Pacific Grove, CA, Oct. 2008, 41–44.

[25] Gogineni, S., and Nehorai, A.
Adaptive design for distributed MIMO radar using sparse modeling.
In *Proceedings of the International Waveform Diversity Design WDD Conference*, Niagara Falls, Canada, Aug. 2010, 23–27.

[26] Eldar, Y. C., Kuppinger, P., and Bolcskei, H.
Block-sparse signals: Uncertainty relations and efficient recovery.
*IEEE Transactions on Signal Processing*, **58** (Jun. 2010), 3042–3054.

[27] Osborne, M. J.
*An Introduction to Game Theory*. New York: Oxford University Press, 2003.

[28] CVX: Matlab software for disciplined convex programming, version 1.21. http://cvxr.com/cvx, Apr. 2011.

[29] Grant, M., and Boyd, S.
Graph implementations for nonsmooth convex programs.
In *Recent Advances in Learning and Control*, ser. Lecture Notes in Control and Information Sciences, V. Blondel, S. Boyd, and H. Kimura, Eds. Springer-Verlag Limited, 2008, 95–110.

[30] Malioutov, D., Cetin, M., and Willsky, A. S.
A sparse signal reconstruction perspective for source localization with sensor arrays.
*IEEE Transactions on Signal Processing*, **53** (Aug. 2005), 3010–3022.

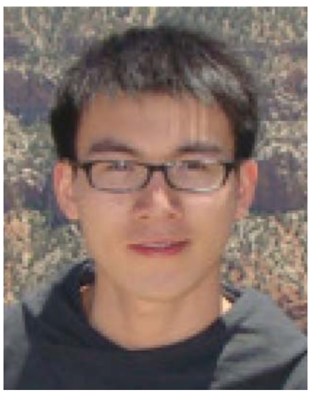

**Keyong Han** (S'12) received the B.Sc. degree in electrical engineering from University of Science and Technology of China in 2010. After that, he received the M.Sc. degree and Ph.D. degree in electrical engineering from Washington University in St. Louis, under the guidance of Dr. Arye Nehorai, in 2012 and 2015, respectively. His research interests include statistical signal processing, radar systems, array processing, and tensor decomposition.

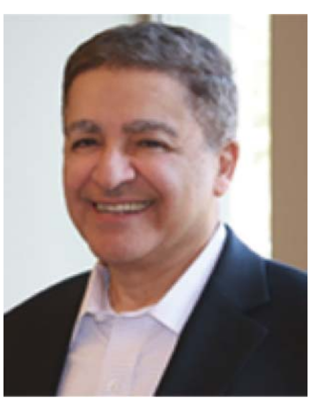

**Arye Nehorai** (S'80–M'83–SM'90–F'94) is the Eugene and Martha Lohman Professor and Chair of the Preston M. Green Department of Electrical and Systems Engineering (ESE), professor in the Department of Biomedical Engineering (by courtesy) and in the Division of Biology and Biomedical Studies (DBBS) at Washington University in St. Louis (WUSTL). He serves as director of the Center for Sensor Signal and Information Processing at WUSTL. Under his leadership as department chair, the undergraduate enrollment has more than tripled in the last four years. Earlier, he was a faculty member at Yale University and the University of Illinois at Chicago. He received the B.Sc. and M.Sc. degrees from the Technion, Israel, and the Ph.D. degree from Stanford University, California.

Dr. Nehorai served as editor-in-chief of the *IEEE Transactions on Signal Processing* from 2000 to 2002. From 2003 to 2005 he was the vice president (publications) of the IEEE Signal Processing Society (SPS), the chair of the publications board, and a member of the executive committee of this society. He was the founding editor of the special columns on Leadership Reflections in *IEEE Signal Processing Magazine* from 2003 to 2006.

Dr. Nehorai received the 2006 IEEE SPS Technical Achievement Award and the 2010 IEEE SPS Meritorious Service Award. He was elected Distinguished Lecturer of the IEEE SPS for a term lasting from 2004 to 2005. He received several best paper awards in IEEE journals and conferences. In 2001 he was named University Scholar of the University of Illinois. Dr. Nehorai was the principal investigator of the Multidisciplinary University Research Initiative (MURI) project titled Adaptive Waveform Diversity for Full Spectral Dominance from 2005 to 2010. He is a Fellow of the IEEE since 1994, Fellow of the Royal Statistical Society since 1996, and Fellow of AAAS since 2012.